

Published in final edited form as:

Neurosci Lett. 2011 March 29; 492(1): 11–14. doi:10.1016/j.neulet.2011.01.036.

Impaired dopamine release and uptake in R6/1 Huntington's disease model mice

Andrea N. Ortiz^a, Benjamin J. Kurth^a, Gregory L. Osterhaus^a, and Michael A. Johnson^{a,b}

^aDepartment of Chemistry and R. N. Adams Institute of Bioanalytical Chemistry, Lawrence, KS 66045 USA

^bNeuroscience Program, Lawrence, KS 66045 USA

Abstract

Huntington's disease (HD) is a progressive, neurodegenerative movement disorder. Here, we used fast-scan cyclic voltammetry to measure dopamine release and uptake in striatal brain slices from R6/1 HD model mice. Peak dopamine release ($[DA]_{max}$) was significantly diminished in R6/1 mice (52% of wild-type at 24 weeks of age). Similarly, dopamine released per locally applied electrical stimulus pulse ($[DA]_p$), which is $[DA]_{max}$ corrected for uptake and electrode performance, was also diminished in R6/1 mice (43% of wild-type by 24 weeks of age). Moreover, V_{max} , the maximum rate of dopamine uptake, obtained by modeling the stimulated release plots, was decreased at 16 and 24 weeks of age in R6/1 mice (51 and 48% of wild-type, respectively). Thus, impairments in both dopamine release and uptake appear to progress in an age-dependent manner in R6/1 mice.

Keywords

dopamine; voltammetry; Huntington's disease; R6/1 mice; release; uptake

Introduction

Huntington's disease (HD) is an autosomal dominant neurodegenerative disorder caused by an expanded CAG repeat on the gene that encodes the *huntingtin* (*htt*) protein [1]. This expansion results in the expression of an extended polyglutamine segment, ultimately resulting in striatal degeneration, mood disturbances, choreic movements, and cognitive dysfunction [2]. Dopaminergic innervation projecting from the substantia nigra pars compacta to the striatum exerts influence over the control of intentional movement [3]. Therefore, it has been suggested that impairments in dopamine (DA) release may contribute to the progressive motor phenotype that is characteristic of HD [4–6].

Several genetically engineered mouse strains that model HD have been used to investigate dopaminergic system alterations. Of these, the R6/2 mouse, which possesses exon 1 of the human huntingtin (*htt*) protein with about 144 CAG repeats [7–8], has been the most extensively studied. R6/2 mice express a progressive, overt behavioral phenotype that starts between 9 to 11 weeks of age and typically die at 10 to 13 weeks of age [7–8]. In contrast, R6/1 mice, which also express a truncated version of the human *htt*, have a shorter CAG

To whom correspondence should be addressed: Michael A. Johnson, The University of Kansas, Department of Chemistry, 1251 Wescoe Hall Drive, 2010 Malott Hall, Lawrence, KS 66047-7572, Telephone: (785) 864-4629, Fax: (785) 864-4629, johnsonm@ku.edu.

repeat length of about 116 repeats. Thus, overt phenotype onset begins later in life at 15 to 21 weeks of age with death occurring between 32 and 40 weeks of age [8].

Dopamine release, measured by fast-scan cyclic voltammetry (FSCV) at carbon-fiber microelectrodes, has been shown to be impaired in striatal brain slices from R6/2 mice, while uptake was unchanged [5]. However, studies in which exocytotic DA release was directly measured in R6/1 mice have not been reported to our knowledge, although recent evidence raises the possibility that dopamine system function is indeed altered. Increases in extracellular DA induced by ip injection of malonate, an excitotoxin, are less in R6/1 mice compared to wild-type (WT) control mice even though DA content, measured in striatal lysates, is unchanged [9-10]. Moreover, R6/1 mice exhibit a blunted locomotor response to amphetamine, but not apomorphine, indicating that presynaptic dysfunction of the dopaminergic system is responsible for these behavioral alterations [10]. Nevertheless, it is not known if DA release and uptake are altered. A clear assessment of DA release and uptake dynamics in R6/1 mice and other HD model rodents is important because underlying genetic differences, such as CAG repeat length, may alter nervous system function differently between strains.

In this work, we used FSCV to investigate DA release and uptake in striatal brain slices harvested from R6/1 mice. FSCV is useful in this case because its good temporal resolution (10 measurements/s as applied in this work) allows for DA release and uptake to be measured as separate processes.

Material and Methods

Animals

R6/1 [CBy.Cg-Tg(HDexon1)61b] and non-carrier control wild-type (WT) mice were purchased from Jackson Laboratories (Bar Harbor, Maine) and were housed at the University of Kansas animal care unit prior to use. Food and water were provided ad libitum and a 12-hour light-dark cycle was used. All animal procedures were approved by the University of Kansas Institutional Animal Care and Use Committee.

Brain Slice Preparation

Brain slices were prepared, as previously described, from R6/1 and WT mice at 10, 16, and 24 weeks of age [5]. Mice were anesthetized by isoflurane inhalation and then decapitated. The brain was immediately removed and placed in ice cold artificial cerebrospinal fluid (aCSF) consisting of 126 mM NaCl, 2.5 mM KCl, 1.2 mM NaH₂PO₄, 2.4 mM CaCl₂, 1.2 mM MgCl₂, 25 mM NaHCO₃, 20 mM HEPES, and 11 mM D-Glucose with a pH of 7.4. The aCSF was oxygenated by bubbling 95% O₂/5% CO₂ gas into the aCSF throughout the experiment. After the brain was removed from the skull, the cerebellum was sliced off and the brain was mounted on an aluminum block. Coronal slices, 300 μm thick, were made using a vibratome slicer (Leica, Wetzlar, Germany). A single brain slice was placed in the superfusion chamber, which was maintained at 34°C and had a continuous flow of aCSF at a rate of 2 mL/min. Each brain slice was equilibrated in the superfusion chamber for 60 minutes prior to obtaining measurements.

DA release in brain slices

Carbon-fiber microelectrodes were fabricated as previously described [4]. Briefly, a single 7 μm diameter carbon-fiber (Goodfellow Cambridge Ltd, Huntingdon, U.K.) was aspirated through a glass capillary tube (1.2 mm outer diameter, 0.68 mm inner diameter, 4 inches long, A-M Systems, Inc. Carlsborg, WA, USA), and then the capillary tube was pulled using a heated coil puller (Narishige International USA, Inc., East Meadow, NY). After the

electrodes were trimmed to about 25 μm from the glass seal they were further insulated with epoxy resin (EPON resin 815C, EPIKURE 3234 curing agent, Miller-Stephenson, Danbury, CT, USA), and then cured at 100°C for 1 h. The electrodes were backfilled with 0.5 M potassium acetate in order to provide an electrical connection between the carbon fiber and an inserted silver wire.

A triangular waveform was applied to the carbon-fiber working electrode. The potential was held -0.4 V, increased to $+1.0$ V, and then scanned back to -0.4 V at a scan rate of 300 V/s and an update rate of 60 Hz. A headstage amplifier was interfaced with a computer via a breakout box and custom software provided by R.M. Wightman and M.L.A.V. Heien, University of North Carolina, Chapel Hill. A chlorided silver wire was used as an Ag/AgCl reference electrode. The carbon fiber microelectrode was inserted to a depth of 100 μm in the dorsolateral caudate-putamen region of the striatum between the prongs of a bipolar stimulation electrode (Plastics One, Roanoke, VA), which was separated by a distance of 200 μm . A single electrical stimulus pulse at 60Hz was applied to the brain slice and the current was then measured at the peak oxidation potential for dopamine (about $+0.6\text{V}$ versus Ag/AgCl reference electrode). Working electrodes were calibrated in a flow cell before and after each use with dopamine standards of known concentration. These dopamine standards were prepared by dissolving 3-hydroxytyramine hydrobromide, 99% (Sigma-Aldrich, St. Louis, MO) solid in glucose-free aCSF. The temperature of the solutions during analysis was 21 to 24°C. The average of the pre- and post-calibration measurements was used as the calibration factor.

DA release measurements were collected in four locations of the dorsal lateral striatum in each brain slice. Each release plot was then modeled using simplex minimization [11] as previously described in Johnson et al., 2006 [5] to determine $[\text{DA}]_p$, the peak DA release per electrical stimulus pulse, and V_{max} , the maximum uptake rate of DA by the dopamine transporter. K_M was fixed at 0.2 μm during this modeling operation. $[\text{DA}]_p$ is distinguished from $[\text{DA}]_{\text{max}}$, the peak DA release amplitude, because it is corrected for uptake and electrode performance. Values obtained from the four sampling points were used to obtain an average value for each slice.

Statistics

All values are represented as the average \pm SEM, where n = the number of brain slices. Statistical comparisons were made by two-way ANOVA and Bonferroni post-tests on log-transformed data with GraphPad Prism 4.03 software (GraphPad Software, Inc., La Jolla, CA).

Results

DA release was measured using a single pulse stimulation and FSCV at carbon-fiber microelectrodes in brain slices harvested from R6/1 and WT mice at 10, 16, and 24 weeks old (representative data shown in Fig. 1A). Cyclic voltammograms (CVs) obtained at the highest point of stimulated release were used to verify that the analyte detected was DA. The average values of $[\text{DA}]_{\text{max}}$ (Fig. 1B) were: 10 weeks of age, 0.82 ± 0.17 μM (R6/1; $n = 9$ slices from 3 mice) and 0.89 ± 0.14 μM (WT; $n = 8$ slices from 2 mice); 16 weeks of age, 1.03 ± 0.17 μM (R6/1, $n = 16$ slices from 4 mice) and 1.50 ± 0.23 μM (WT, $n = 8$ slices from 2 mice); and 24 weeks of age, 0.48 ± 0.13 μM (R6/1, $n = 8$ slices from 3 mice) and 0.92 ± 0.14 μM (WT, $n = 15$ slices from 5 mice). Statistical analyses by two-way ANOVA revealed significant genotype ($F_{1,56} = 7.45$, $p < 0.01$) and age ($F_{2,56} = 6.53$, $p < 0.005$) effects on $[\text{DA}]_{\text{max}}$. Peak stimulated DA release ($[\text{DA}]_{\text{max}}$) was less in R6/1 mice than WT control mice at 24 weeks of age ($p < 0.05$).

From inspection of individual raw data release plots, it appeared that the concentration of evoked DA decreased at a slower rate in slices from R6/1 mice than in slices from age-matched WT mice at 16 and 24 weeks of age. This observation prompted us to model the curves in order to calculate V_{\max} and $[DA]_p$ (Fig. 2A). Similar to the trend observed with $[DA]_{\max}$, genotype ($F_{1,56} = 8.03$, $p < 0.01$) and age ($F_{2,56} = 4.59$, $p < 0.05$) significantly interacted with $[DA]_p$ (Fig. 2B). The average values of $[DA]_p$ were: 10 weeks of age, $1.58 \pm 0.44 \mu\text{M}$ (R6/1) and $1.67 \pm 0.30 \mu\text{M}$ (WT); 16 weeks of age, $1.45 \pm 0.21 \mu\text{M}$ (R6/1) and $2.13 \pm 0.36 \mu\text{M}$ (WT); and 24 weeks of age, $0.66 \pm 0.14 \mu\text{M}$ (R6/1) and $1.53 \pm 0.27 \mu\text{M}$ (WT). By 16 weeks of age, $[DA]_p$, although not significant, appeared to be less in R6/1 mice than in WT mice. At 24 weeks of age, the R6/1 mice released significantly less ($p < 0.05$) DA than age-matched WT control mice. Additionally, R6/1 mice released less DA at 16 weeks of age than R6/1 mice at 24 weeks of age ($p < 0.05$).

The data obtained from the aforementioned modeling operation also provided us with V_{\max} . The average values of V_{\max} were: 10 weeks of age, $10.5 \pm 4.3 \mu\text{M/s}$ (R6/1) and $9.0 \pm 2.3 \mu\text{M/s}$ (WT); 16 weeks of age, $4.12 \pm 0.55 \mu\text{M/s}$ (R6/1) and $8.08 \pm 1.99 \mu\text{M/s}$ (WT); and 24 weeks of age, $3.13 \pm 0.98 \mu\text{M/s}$ (R6/1) and $6.52 \pm 1.74 \mu\text{M/s}$ (WT). Genotype significantly interacted with V_{\max} ($F_{1,58} = 4.47$, $p < 0.05$) (Fig. 2C).

Discussion

In this study, we examined DA release and uptake in R6/1 mice at 10, 16, and 24 weeks of age. $[DA]_p$ and V_{\max} were determined from the best-fit parameters that were used in modeling the stimulated release plots. These results show that $[DA]_{\max}$, $[DA]_p$, and V_{\max} decrease progressively over time compared to age-matched WT mice.

Our initial results indicated that $[DA]_{\max}$, the peak concentration of evoked DA detected at the electrode, progressively decreased in R6/1 mice as they aged. Therefore, we modeled the plots to determine $[DA]_p$ and V_{\max} . $[DA]_p$ may be considered a more reliable measure of how much DA is released per electrical stimulus pulse because it takes into account DA uptake and electrode performance. $[DA]_p$ also decreased with age and was significantly diminished by 24 weeks. Complementary to our results are previous microdialysis studies which show that basal DA levels and malonate-induced DA efflux are diminished in the R6/1 striatum [12] even though striatal DA content is unchanged at either 16 weeks [12] or 30 weeks of age [10]. Therefore, the $[DA]_p$ values obtained using FSCV allow us to make the more specific interpretation that the ability of dopaminergic terminals to release DA by exocytosis is progressively impaired in R6/1 mice. These findings are similar to those found in R6/2 mice [5]; however, consistent with having a shorter CAG repeat length, this impairment progresses more slowly with age.

In addition to DA release, values of V_{\max} were decreased in R6/1 mice compared to WT control mice. Previous labeling experiments indicate that striatal DAT expression is similar in R6/1 and WT littermate mice [9]. Thus, decreased uptake is likely not related to a decrease in the number of DAT protein molecules. This determination is important because DA uptake by the DAT is known to follow Michaelis-Menten uptake kinetics and, therefore, the equation $V_{\max} = k_{\text{cat}}[E]_t$ is obeyed, where k_{cat} is a rate constant and $[E]_t$ represents the total enzyme concentration [13], in this case DAT. Thus, since $[E]_t$ is likely unchanged, the difference in uptake may represent a modification of the transporter or a change in its availability on the membrane surface. Indeed, D2 autoreceptor activation has been shown to up-regulate DAT function [14]; nevertheless, it is unclear why V_{\max} is apparently unaffected in R6/2 mice throughout the entire course of phenotype progression [5].

In conclusion, this report reveals key malfunctions in DA release in R6/1 mice, and also shows that the DA uptake kinetics of R6/1 differ from those of R6/2 mice, a popularly used genetic HD model. These findings reveal potentially important considerations for researchers studying DA system function in these HD models.

Acknowledgments

This work was funded by the Huntington's Disease Society of America, NIH P20 RR016475 from the INBRE Program of the National Center for Research Resources, and The University of Kansas.

References Cited

- [1]. The Huntington's Disease Collaborative Research Group. A novel gene containing a trinucleotide repeat that is expanded and unstable on Huntington's disease chromosomes. *Cell*. 1993; 72(6): 971–83. [PubMed: 8458085]
- [2]. Bates, GP.; Harper, PS.; Jones, L. Huntington's Disease. Oxford University Press; Oxford; 2002. p. 558
- [3]. Kandel, ER.; Schwartz, JH.; Jessell, TM. Principles of Neural Science. McGraw-Hill; New York; 2000.
- [4]. Kraft JC, Osterhaus GL, Ortiz AN, Garris PA, Johnson MA. In vivo dopamine release and uptake impairments in rats treated with 3-nitropropionic acid. *Neuroscience*. 2009; 161:940–949. [PubMed: 19362126]
- [5]. Johnson MA, Rajan V, Miller CE, Wightman RM. Dopamine release is severely compromised in the R6/2 mouse model of Huntington's disease. *J Neurochem*. 2006; 97:737–746. [PubMed: 16573654]
- [6]. Ortiz AN, Kurth BJ, Osterhaus GL, Johnson MA. Dysregulation of intracellular dopamine stores revealed in the R6/2 mouse striatum. *J Neurochem*. 2010; 112:755–761. [PubMed: 19929911]
- [7]. Davies SW, Turmaine M, Cozens BA, DiFiglia M, Sharp AH, Ross CA, Scherzinger E, Wanker EE, Mangiarini L, Bates GP. Formation of neuronal intranuclear inclusions underlies the neurological dysfunction in mice transgenic for the HD mutation. *Cell*. 1997; 90:537–548. [PubMed: 9267033]
- [8]. Mangiarini L, Sathasivam K, Seller M, Cozens B, Harper A, Hetherington C, Lawton M, Trotter Y, Lehrach H, Davies SW, Bates GP. Exon 1 of the HD gene with an expanded CAG repeat is sufficient to cause a progressive neurological phenotype in transgenic mice. *Cell*. 1996; 87:493–506. [PubMed: 8898202]
- [9]. Petersén A, Puschban Z, Lotharius J, NicNiocail B, Wiekop P, O'Connor WT, Brundin P. Evidence for dysfunction of the nigrostriatal pathway in the R6/1 line of transgenic Huntington's disease mice. *Neurobiol Dis*. 2002; 11:134–146. [PubMed: 12460553]
- [10]. Pineda JR, Canals JM, Bosch M, Adell A, Mengod G, Artigas F, Ernfors P, Alberch J. Brain-derived neurotrophic factor modulates dopaminergic deficits in a transgenic mouse model of Huntington's disease. *J Neurochem*. 2005; 93:1057–1068. [PubMed: 15934928]
- [11]. Wu Q, Reith ME, Wightman RM, Kawagoe KT, Garris PA. Determination of release and uptake parameters from electrically evoked dopamine dynamics measured by real-time voltammetry. *J Neurosci Methods*. 2001; 112:119–33. [PubMed: 11716947]
- [12]. Petersén A, Hansson O, Puschban Z, Sapp E, Romero N, Castilho RF, Sulzer D, Rice M, DiFiglia M, Przedborski S, Brundin P. Mice transgenic for exon 1 of the Huntington's disease gene display reduced striatal sensitivity to neurotoxicity induced by dopamine and 6-hydroxydopamine. *Eur J Neurosci*. 2001; 14:1425–1435. [PubMed: 11722604]
- [13]. Mathews, CK.; van Holde, KE. *Biochemistry*. Benjamin/Cummings; Menlo Park, CA: 1996. p. 1158
- [14]. Bolan EA, Kivell B, Jaligam V, Oz M, Jayanthi LD, Han Y, Sen N, Urizar E, Gomes I, Devi LA, Ramamoorthy S, Javitch JA, Zapata A, Shippenberg TS. D2 receptors regulate dopamine transporter function via an extracellular signal-regulated kinases 1 and 2-dependent and phosphoinositide 3 kinase-independent mechanism. *Mol Pharmacol*. 2007; 71:1222–1232. [PubMed: 17267664]

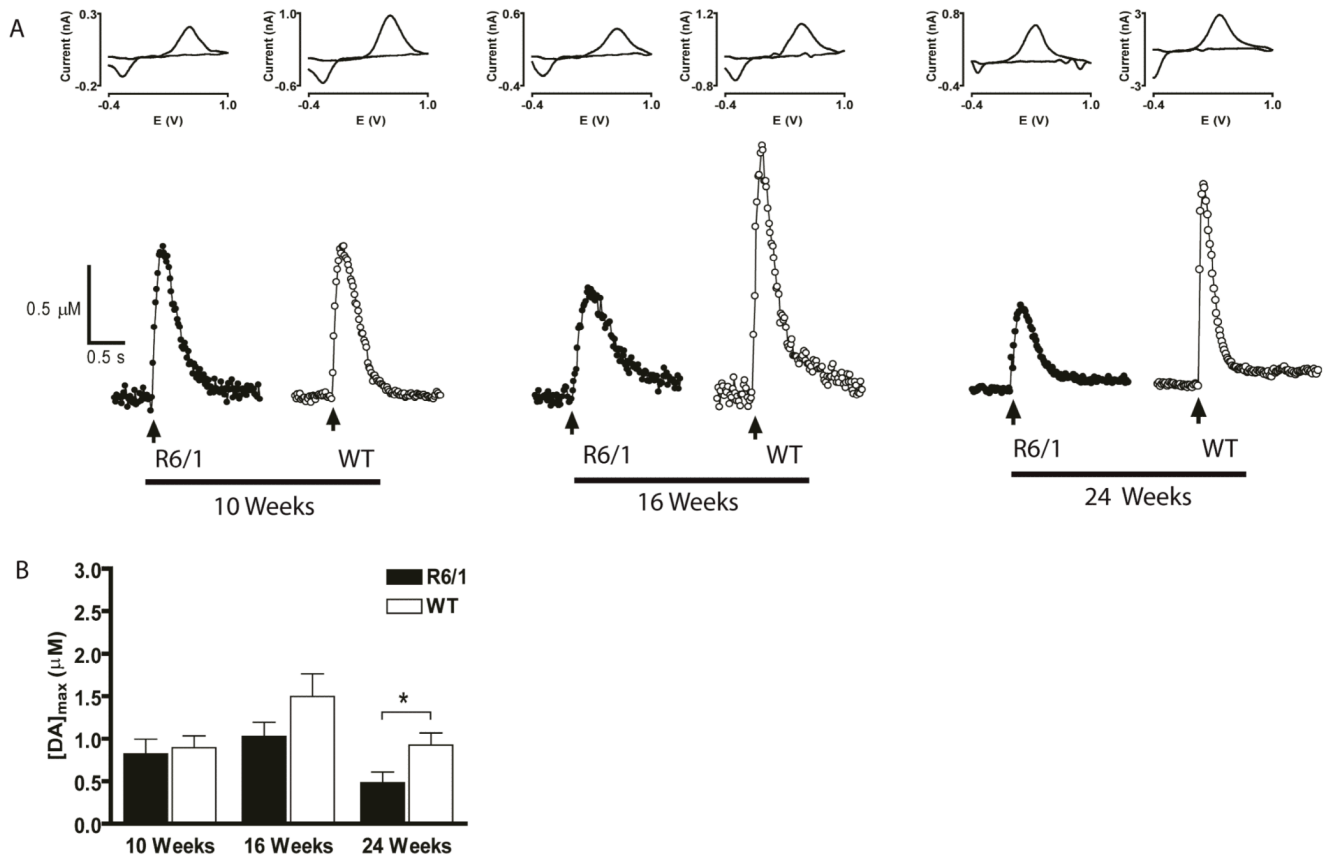


Fig 1. Stimulated DA release is diminished in older R6/1 mice compared to age-matched WT mice. (A) Representative plots of stimulated DA release in striatal brain slices from R6/1 and WT mice. The time at which the electrical stimulus pulse is applied is indicated by the arrow. (B) Bar graph of average $[DA]_{max}$ measured in striatal slices from R6/1 and WT control mice at 10, 16, and 24 weeks of age. $[DA]_{max}$ was significantly diminished in R6/1 mice at 24 weeks of age (* $p < 0.05$, $n = 8$ R6/1 and 15 WT).

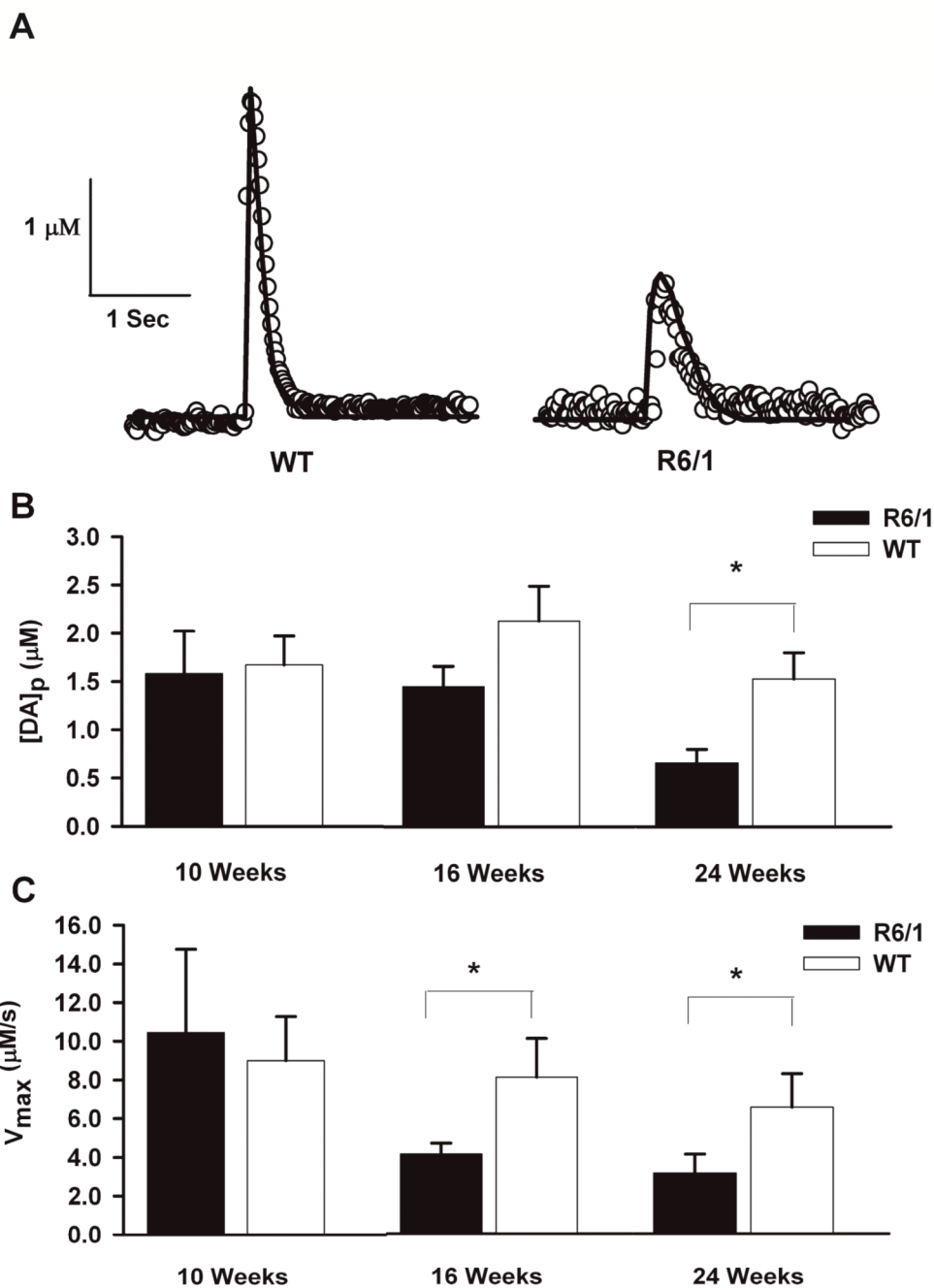


Fig. 2. DA release per pulse $[\text{DA}]_p$ and V_{max} are decreased in R6/1 mice compared to age-matched WT mice. (A) Representative plots and modeled curves of stimulated DA release in striatal brain slices taken from 24-week-old R6/1 and WT mice. (B) and (C), Bar graphs of average $[\text{DA}]_p$ and V_{max} measured in striatal slices from R6/1 and WT control mice at 10, 16, and 24 weeks of age (* $p < 0.05$, $n = 8$ R6/2 and 15 WT).